Published in final edited form as:
Exp Eye Res. 2011 February ; 92(2): 155–160. doi:10.1016/j.exer.2010.10.009.

Spatial correlation of mouse photoreceptor-RPE thickness between SD-OCT and histology

Eric J. Knott[*], **Kristopher G. Sheets**[*], **Yongdong Zhou**, **William C. Gordon**, and **Nicolas G. Bazan**
Neuroscience Center of Excellence and Department of Ophthalmology, Louisiana State University Health Sciences Center, New Orleans, LA

Abstract

Spectral Domain Optical Coherence Tomography (SD-OCT) applied to the mouse retina has been limited due to inherent movement artifacts and lack of resolution. Recently, SD-OCT scans from a commercially available imaging system have yielded retinal thickness values comparable to histology. However, these measurements are based on single point analysis of images. Here we report that using the Spectralis HRA+OCT Spectral Domain OCT and Fluorescein Angiography system (Heidelberg Engineering, Heidelberg, Germany), retinal thickness of linear expanses from SD-OCT data can be accurately assessed. This is possible by the development of a Spectralis-compatible ImageJ plug-in that imports 8-bit SLO and 32-bit OCT B-scan images, retaining scale and segmentation data and enabling analysis and 3-D reconstruction. Moreover, mouse retinal layer thickness values obtained with this plug-in exhibit a high correlation to thickness measurements from histology of the same retinas. Thus, use of this ImageJ plug-in results in reliable quantification of long retinal expanses from *in vivo* SD-OCT images.

Keywords

Spectral Domain Optical Coherence Tomography (SD-OCT); ImageJ plug-in; retina; mouse; retinal thickness; histology

1. Introduction

Classic evaluation of retinal degeneration relies on histological sample preparation and light microscopy, requiring extensive animal numbers, costly embedding materials, days of processing, sectioning, and imaging, and many technician hours. New technology can now be employed that will greatly reduce preparation time and allow longitudinal analysis of single animals throughout extended experimental protocols. Spectral Domain - Optical

Corresponding Author: Nicolas G. Bazan, Neuroscience Center of Excellence, Louisiana State University Health Sciences Center, 2020 Gravier Street, Suite D New Orleans, LA 70112, Tel: (504) 599-0832, Fax: (504) 568-5801, nbazan@lsuhsc.edu.
[*]These authors contributed equally

Knott: initial draft, light damage treatment, all histology sections, histology imaging and measurements, OCT segmentation, data tabulation
Sheets: second draft, wrote the ImageJ plug-in, data tabulation, statistical analysis, figures
Zhou: OCT imaging
Gordon and Bazan: wrote the final draft of the paper

Coherence Tomography (SD-OCT) has emerged as a promising approach to measure retinal thickness and morphological changes *in vivo*. While concerns about the resolution of this technology have been expressed, SD-OCT has enabled accurate imaging of the mouse retina, facilitating longitudinal studies of disease-related retinal alterations (Fischer et al., 2009; Kim et al., 2008; Wolf-Schnurrbusch et al., 2008). Moreover, it has been shown that SD-OCT-derived measurements are analogous to those obtained from histology based upon *single point* measurements from each retina (Fischer et al., 2009; Huber at el., 2009). Here, we report accurate and reproducible measurements of retinal thickness using the *entire* SD-OCT B-scan. In addition, we show that these measurements are comparable to those obtained from conventional histology in light-induced photoreceptor cell loss for mice.

Using Heidelberg Spectralis Viewing Module software, the distance between any two points in an OCT B-scan can be measured manually, or the segmented retinal layer thickness of an individual OCT A-scan can be obtained from the thickness profile. The thickness profile, however, cannot be exported in its entirety, forcing the user to select individual A-scan positions from which to determine the thickness of a layer. Nevertheless, since the equipment provides the ability to export the entire raw Scanning Laser Ophthalmoscope (SLO) image and OCT data in binary format, we designed a custom plug-in for ImageJ to interpret the exported binary files according to the data structure described in *Raw Export Instructions - Spectralis Viewing Module 4.0*.

Since ImageJ software is a freely available, Java-based image processing program developed and distributed by the National Institutes of Health, our plug-in enables the sharing of Heidelberg SD-OCT files with investigators who lack access to Spectralis Viewing Software. Once opened in ImageJ, additional processing with other plug-ins, such as “Straighten” (Kocsis et al. 1991) can be performed to convert desired retinal layers from 3D cross-sectional SD-OCT into 3D pseudo *en-face* SD-OCT (Ishikawa et al., 2009). While it is currently possible to view 3D-OCT files outside of Spectralis software, it requires exporting the information in 8-bit grayscale as an avi formatted movie, which is readable by ImageJ. Since avi files are in 24-bit RGB format, this method, at a minimum, triples the size of the 8-bit image data, making it highly inefficient. As an example, a 3D-OCT file consisting of 145 B-scans was exported as both an avi and raw file. The avi file size was 3,147,229 kilobytes, while the raw file size was 90.7% smaller (292,306 kilobytes).

Also, within Spectralis software, the log of 32-bit OCT data is subsequently presented in 8-bit grayscale and no option, other than raw export, permits viewing the original 32-bit data linearly. The Spectralis raw file contains the original 32-bit data. However, no software currently exists to read the binary format of the raw file. The combination of ImageJ and the plug-in, which we introduce here, represents the first software solution to visualize the original 32-bit Spectralis OCT data. The potential of 32-bit OCT reflectance values has recently been demonstrated, using Adaptive Optics-OCT, to visualize, *in vivo*, the renewal of human cone outer segments (Jonnal et al., 2010). Therefore, our plug-in enables access to 32-bit data, while, at the same time, minimizing file size by more than 90%.

2. Materials and Supplies

Male Balb/c mice (25 g, age-matched within 2 days) were purchased from Charles River (Wilmington, MA). The anesthesia, a ketamine/xylazine mixture (200 mg/kg and 10 mg/kg, respectively) for mice, was supplied by our Louisiana State University Health Sciences Center (LSUHSC) Animal Care Facility veterinarian. Noncorrective contact lenses fitted to the mouse cornea were purchased from Veterinary Speciality Products (Whitechurch, Shropshire, Great Britian), and methyl cellulose (used as a 1% solution to prevent corneal dessication), sodium cacodylate (0.1 M fixation buffer), paraformaldehyde (2% fixative in

buffer), and toluidine blue (1% in sodium borate, to contrast plastic sections) were obtained from Sigma-Aldrich (St Louis, MO). Glutaraldehyde (70% stock solution, used as a 2% fixative in buffer), osmium (1% in buffer for secondary fixation), Epon/araldite plastic embedding kits, and glass strips (microtome knives for 1 μm-thick plastic sections) were obtained from Electron Microscope Supplies (EMS, Hatfield, PA). Sections were mounted on Superfrost Plus microscope slides and viewed through 1 oz 22 × 22 mm coverslips (VWR International, West Chester, PA) floated on glycerin. Images of histologic sections were obtained with a Nikon Plan 20x NA 0.4 objective attached to a Nikon Optiphot-2 microscope, using a Nikon Digital Sight DS-Ri1 digital camera and Nikon NIS Elements v3.0 software, resolution 0.2 μm/pixel, calibrated against a Pyser-Sgi stage micrometer. SD-OCT scans were obtained with the Heidelberg Spectralis HRA+OCT system, and segmented with Heidelberg Spectralis Viewing Module software, v4.0 (Heidelberg Engineering, Heidelberg, Germany). Image analysis was accomplished with NIH ImageJ software (http://imagej.nih.gov/ij/), v1.43n (64 bit) and v1.43o (32 bit), coupled with our custom ImageJ plug-in (available at http://imagej.nih.gov/ij/plugins/heyex/index.html) for segmentation of outer retina thickness.

3. Detailed Methods

Throughout the development of this method all procedures were carried out according to the *Association for Research in Vision and Ophthalmology (ARVO) statement for the Use of Animals in Ophthalmic and Vision Research and the LSUHSC Institutional Animal Care and Use Committee (IACUC).*

We have developed a method that will more accurately measure photoreceptor-RPE thickness in the mouse by SD-OCT, and we test this method on an established retinal degeneration model of bright light treatment that will rapidly eliminate photoreceptors and reduce the outer retina. Initial retinal measurements were established from SD-OCT images and from plastic sections of untreated control mice.

To establish photoreceptor-RPE layer thickness baselines, Balb/c mice (male, 25g) were acclimated seven days under a 12h:12h light cycle (0600 h onset) at an intensity of 40 lux (measured within cages housed in forced air racks) and given mouse chow and water *ad libitum*. Prior to SD-OCT imaging, mice were anesthetized with a mixture of ketamine/xylazine (200 mg/kg + 10 mg/kg, ip), placed in a conical tube with the tip removed to expose the nose and eyes, and wrapped in a warming blanket. Eyes were then dilated with tropicamide and small drops of methyl cellulose (1%) placed on the eyes, followed by placement of non-correcting contact lenses to prevent corneal dessication. Retinas were imaged by SD-OCT along the vertical meridian through the optic disc (superior retina, optic nerve, inferior retina) using a Heidelberg Spectralis HRA+OCT system (Heidelberg Engineering, Heidelberg, Germany). Signal quality was greater than 20 db and scan speed was 40,000 A-scans per second. Eye motion artifacts were eliminated by in-system eye tracking and at least 25 frames were averaged per B-scan to increase the signal-to-noise ratio. Axial resolution was 7 μm optical and 3.5 μm digital. Mice were then allowed to recover in their cages and returned to the animal care facility.

After two days, mice underwent bright light treatment. Eyes were dilated with drops of tropicamide and each mouse placed in aluminum foil-covered, 12-inch, clear Lucite cubes, open at the top, for six hours. An array of white fluorescent bulbs (Philips, F20T12/CW, 20 Watts) was suspended above at a distance that provided 4000 lux (Ash et al., 2009), measured at the bottom of the Lucite cubes with a LI-COR light meter (Model LI-189 with photometric probe; Lincoln, NB). Another set of control mice were not bright light treated. All animals were allowed eight hours of dark recovery followed by 10 days of normal cyclic

light, after which the final SD-OCT imaging was achieved. Mice were prepared and SD-OCT imaging was conducted as described above.

Immediately after SD-OCT, eyes were collected and prepared for histological imaging and measurements of photoreceptor-RPE layer thicknesses by microscopy. Prior to removal, the superior edge of each eye was marked with a fine tipped permanent marker. After removal, corneas were slit and eyes placed in 2% paraformaldehyde and 2% glutaraldehyde in 0.1 M sodium cacodylate buffer overnight at 4° C. Eyes were then hemi-sected along the vertical meridian through the optic nerve, the lenses removed, and the corneas notched near the superior edge for orientation purposes. Following rinsing, secondary fixation in buffered 1% OsO_4, final rinsing, and dehydration, tissue was embedded in Epon-Araldite plastic for 1 μm-thick toluidine blue-stained sections.

SD-OCT accumulates reflectance data from within the retina to generate an image of an *in vivo* section. This is accomplished by measuring reflectance at sequential depths in the retina at a single location, or A-scan. A lateral expanse of A-scans creates a retinal section referred to as a B-scan. To obtain measurements from the B-scan, layer lines automatically defined by Heidelberg software were manually adjusted. We used this process of *segmentation* to delineate Bruch's membrane and the base of the photoreceptors, and then obtained the distance between them, the outer retina (OR), along the entire B-scan. OR thickness, measured from the base of the photoreceptors to Bruch's membrane in SD-OCT images and their corresponding histologic sections, is shown in Fig 1A. In SD-OCT, OR thickness was calculated at every A-scan position (0.6635 μm) while histologic measurements were made at 20 μm intervals along the entire span of the retina.

To calibrate the optical dimension of the A-scan, corneal curvature values were adjusted until measured optic nerve width was equivalent between SD-OCT and histology. The average curvature used for all OCTs was 0.672 mm, producing an optical resolution of 0.6635 μm/pixel. The OR in SD-OCT was then segmented and raw files exported using Heidelberg Spectralis Viewing Module software (v4.0) (Fig 1A). Segmented OR thickness was obtained using our custom ImageJ plug-in by calculating the vertical distance between Bruch's membrane and the base of the photoreceptors. For statistics, SD-OCT B-scans and histologic measurements were interpolated at 25 μm increments to 875 μm from the optic nerve. All measurements were taken by one examiner blind to treatment conditions. To establish observer error, one retina from each condition was measured three times; repeated measure error was 3.5 μm (data not shown). Correlation was determined by simple linear regression using SAS (v9.1).

Our ImageJ plug-in successfully imports both 8-bit SLO and 32-bit SD-OCT images, retaining pixel scale (optical and SD-OCT), segmentation data, and B-scan position relative to the SLO image. In addition to single B-scan SD-OCT images, the plug-in also opens multiple B-scan SD-OCT images as a stack, enabling 3-D reconstruction, analysis, and modeling. The plug-in is compatible with Spectralis Viewing Module exporting raw data in HSF-OCT-101 format. Scan patterns of single line, volume in ART mode, and fast volume, were all successfully tested.

OR thickness in naïve and light-treated mice revealed a high correlation between SD-OCT and histomorphometric analysis. Prior to bright light exposure, mice exhibited a mean OR thickness of 115.0 ± 5.0 μm by SD-OCT. It was also noted that occasional, newly-acquired, untreated mice exhibited signs of moderate retinal degeneration upon initial SD-OCT examination (data not shown), illustrating an advantage of using SD-OCT in longitudinal studies over conventional histomorphometry. Following 10 days of cycled ambient room light, naïve controls exhibited no photoreceptor degeneration, with a mean OR thickness of

114.9 μm ± 5.0 μm by SD-OCT. A near identical value was obtained from histologic sections (117.0 ± 7.0 μm) (Fig 1B). Mice exposed to six hours bright light, followed by 10 days of recovery, exhibited reduced OR thickness in both inferior and superior hemispheres (Fig 2); SD-OCT revealed a mean OR thickness of 72.3 ± 5.0 μm, while histology exhibited a mean thickness of 75.9 μm and a larger standard error of 7.1 μm (Fig 1B). Direct comparison of OR thickness between SD-OCT and histomorphometry yielded a high overall correlation ($R^2 = 0.8518$) (Fig 3, left inset). When correlation was evaluated against distance from the optic nerve, it was shown that the correlation was lowest in vicinity of the optic nerve (Fig 3). By conventional histomorphometry, mean OR thickness near the optic nerve was indistinguishable between groups (Fig 1C), whereas SD-OCT analysis clearly discriminated these points (Fig 1D). Excluding thickness values below the first 200 micrometers from the optic nerve increased the overall correlation to 0.9042 (Fig 3, right inset).

4. Potential Pitfalls and Trouble Shooting

The optical dimensions of the A-scan are calculated by the refractive power of the imaged eye. The majority of refraction in humans is performed by the cornea. Accordingly, Spectralis uses corneal curvature to determine the A-scan's optical resolution. The mouse, however, does not rely on the cornea as the principle refractive element. Moreover, the refractive properties of the mouse eye are known to change with age (Schumaker and Schaeffel, 2004). A single average curvature value was permissible in the present study since the longitudinal duration was brief (12 days elapsed time) and minimal age difference existed among mice. In longitudinal studies of 30 days or greater, or if significant age differences exist, some method of correcting corneal curvature values for age-related changes in refractive properties of the mouse eye is suggested.

When analyzing retinal thickness by OCT and histology, the low correlation observed near the optic nerve may result from three possible sources of error. If the eye is not sectioned sagitally along the vertical meridian passing through the optic nerve, sections will be slightly oblique and retinal thickness measurements can be inflated. This error is minimized by observing the number of nuclei (the thickness) in the outer nuclear layer (ONL) and correcting the tissue block orientation to produce the shortest dimension (e.g., in normal mice, 10–11 nuclei in ONL thickness is usual, while 14–15 nuclei indicates obliqueness). Also, long Müller cell processes are apparent in well oriented sections. Similar misalignment can occur with SD-OCT. However, if the eye is oriented at an angle, the OCT optics will be unable to capture a high quality image. Thus, we used an acceptance criteria of 20 db for B-scans. Secondly, during SD-OCT imaging, the animal must be positioned with the superior retina located at the upper-most position. This rotational error around the optical axis of the eye can also be induced during histologic sectioning. While alignment in both techniques is approximated visually, there is no precise method to ensure exact alignment. Finally, incorrect lateral registration during SD-OCT and subsequent histology of the same retina can induce errors. The histological section must be at the same location from which the OCT B-scan was acquired. The ability, or inability, to find the exact position twice will determine the accuracy of the lateral registration, and may possibly account for the greatest source of error. We attempt to acquire both SD-OCT and histological images through the center of the optic nerve, but the optic nerve is 200 um wide and determining when a section passes through the midline is difficult. One solution to minimize registration error during this process is to acquire SD-OCT in three dimensions, re-orient the 3D volume, and resection to register the B-scan to the histologic section. A recent study of the monkey retina with SD-OCT details this problem and introduces this method of registration (Strouthidis et al., 2010).

Tissue processing will also induce distortions. The high osmolarity of 4% formaldehyde fixation has been shown to cause volume contraction of whole eyes, while immersion fixation in formaldehyde/glutaraldehyde diminishes distortion (Margo and Lee, 1995). Concerns over long duration retinal fixation and possible tissue distortions have been expressed, and this was addressed in a study of donor retinas of 17–95 years of age that had been in fixative for 4 days to 6 years (Gao and Hollyfield, 1992). Also, reduction of intraocular pressure in human patients with IOP >28 mm Hg caused a reduction in the mean cup volume of the optic nerve head one hour after treatment (Meredith et al., 2007), demonstrating that IOP may be important in maintaining structural integrity around the optic nerve. These studies suggest that removal of an experimental eye, followed by a corneal slit and immersion in fixative, may suddenly induce inward movement of the retina near the optic nerve. Thus, comparisons of retinal thickness obtained from histological sections and from *in vivo* SD-OCT images may show difference that are related to preparation methods and duration of fixation.

While these sources of variability may account for differences near the optic nerve, it seems unlikely that preparation or fixation methods are factors since histological and SD-OCT measurements of OR thickness in control animals are very similar. The greatest variation near the optic nerve is found in light-induced degenerating retinas, suggesting an effect associated with the degenerative process. When animals undergo light-induced retinal degeneration, not all respond equally, resulting in variability of the position and size of the damaged area. In fact, the damaged region can occur within the superior retina alone, or extend past the optic nerve into the inferior retina, and is diagonally oriented with the inferior-most edge in the nasal quadrant (Cortina et al., 2005). Since the transition zone is not perpendicular to the vertical meridian used for SD-OCT and histologic orientation, errors in registration produce greater OR thickness variability and would account for the observed variation near the optic nerve in light- induced degeneration.

In this study, we created an ImageJ plug-in that opens Spectralis raw files, retaining scale and segmentation data from 8-bit SLO and 32-bit SD-OCT images, permitting full-length thickness analysis and 3-D reconstruction from B-scan image stacks. Mouse OR thickness values obtained with this plug-in were highly correlated with thickness measurements taken from histologic sections of the same retinas. Correlation of OR thickness was highest between 200 μm and 875 μm from the optic nerve in both the superior and inferior retina. These results demonstrate that Spectralis SD-OCT combined with our ImageJ plug-in produces precise and accurate measurements of mouse outer retina thickness across long expanses. Therefore, we conclude that SD-OCT can be utilized to reliably follow the progression of retinal degeneration within individual mice. Furthermore, in the case of variable degenerative onset, SD-OCT can be used to register individual retinal degeneration within an experimental set.

Acknowledgments

The authors would like to thank Wayne Rasband of the Research Services Branch, NIMH/NIH, for adding our plug-in to the ImageJ web site, and Cornelius E. Regan, Jr. for his invaluable histological expertise. We would especially like to acknowledge Heidelberg Engineering for trouble shooting our OCT equipment and for their technical assistance in optimizing our application of the HRA+OCT system for small rodent retinal imaging, without which this work would not have been possible. This research was supported by grants from the National Institutes of Health, NCRR (P20 RR016816) and NEI (R01 EY005121), and the Foundation Fighting Blindness (TA-NP-0808-0463-LSUNO).

References

Cortina MS, Gordon WC, Lukiw WJ, Bazan NG. Oxidative stress-induced retinal damage up-regulates DNA polymerase gamma and 8-oxoguanine-DNA-glycosylase in photoreceptor synaptic mitochondria. Exp Eye Res. 2005; 81:742–750. [PubMed: 15979612]

Fischer MD, Huber G, Beck SC, Tanimoto N, Muehlfriedel R, Fahl E, Grimm C, Wenzel A, Reme CE, van de Pavert SA, Wijnholds J, Pacal M, Bremner R, Seeliger MW. Noninvasive, in vivo assessment of mouse retinal structure using optical coherence tomography. PLoS One. 2009; 4:e7507. [PubMed: 19838301]

Gao H, Hollyfield JG. Aging of the human retina. Invest Ophthalmol Vis Sci. 1992; 33:1–17. [PubMed: 1730530]

Huber G, Beck SC, Grimm C, Sahaboglu-Tekgoz A, Paquet-Durand F, Wenzel A, Humphries P, Redmond TM, Seeliger MW, Fischer MD. Spectral domain optical coherence tomography in mouse models of retinal degeneration. Invest Ophthalmol Vis Sci. 2009; 50:5888–5895. [PubMed: 19661229]

Ishikawa H, Kim J, Friberg TR, Wollstein G, Kagemann L, Gabriele ML, Townsend KA, Sung KR, Duker JS, Fujimoto JG, Schuman JS. Three-dimensional optical coherence tomography (3D-OCT) image enhancement with segmentation-free contour modeling C-mode. Invest Ophthalmol Vis Sci. 2009; 50:1344–1349. [PubMed: 18952923]

Jonnal RS, Besecker JR, Derby JC, Kocaoglu OP, Cense B, Gao W, Wang Q, Miller DT. Imaging outer segment renewal in living human cone photoreceptors. Opt Express. 2010; 18:5257–5270. [PubMed: 20389538]

Kim KH, Puoris'haag M, Maguluri GN, Umino Y, Cusato K, Barlow RB, de Boer JF. Monitoring mouse retinal degeneration with high-resolution spectral-domain optical coherence tomography. J Vis. 2008; 8:17.1–17.11. [PubMed: 18318620]

Kocsis E, Trus BL, Steer CJ, Bisher ME, Steven AC. Image averaging of flexible fibrous macromolecules: the clathrin triskelion has an elastic proximal segment. J Struct Biol. 1991; 107:6–14. [PubMed: 1817611]

Margo CE, Lee A. Fixation of whole eyes: the role of fixative osmolarity in the production of tissue artifact. Graefe's Arch Clin Exp Ophthalmol. 1995; 233:366–370.

Meredith SP, Swift L, Eke T, Broadway DC. The acute morphologica changes that occur at the optic nerve head induced by medical reduction of intraocular pressure. J Glaucoma. 2007; 16:556–561. [PubMed: 17873718]

Schumaker, Schaeffel. A paraxial schematic eye model for the growing C57BL/6 mouse. Vision Res. 2004; 44:1857–67. [PubMed: 15145680]

Strouthidis NG, Grimm J, Williams GA, Cull GA, Wilson DJ, Burgoyne CF. A comparison of optic nerve head morphology viewed by spectral domain optical coherence tomography and by serial histology. Invest Ophthalmol Vis Sci. 2010; 51:1464–1474. [PubMed: 19875649]

Wolf-Schnurrbusch UE, Enzmann V, Brinkmann CK, Wolf S. Morphologic changes in patients with geographic atrophy assessed with a novel spectral OCT-SLO combination. Invest Ophthalmol Vis Sci. 2008; 49:3095–3099. [PubMed: 18378583]

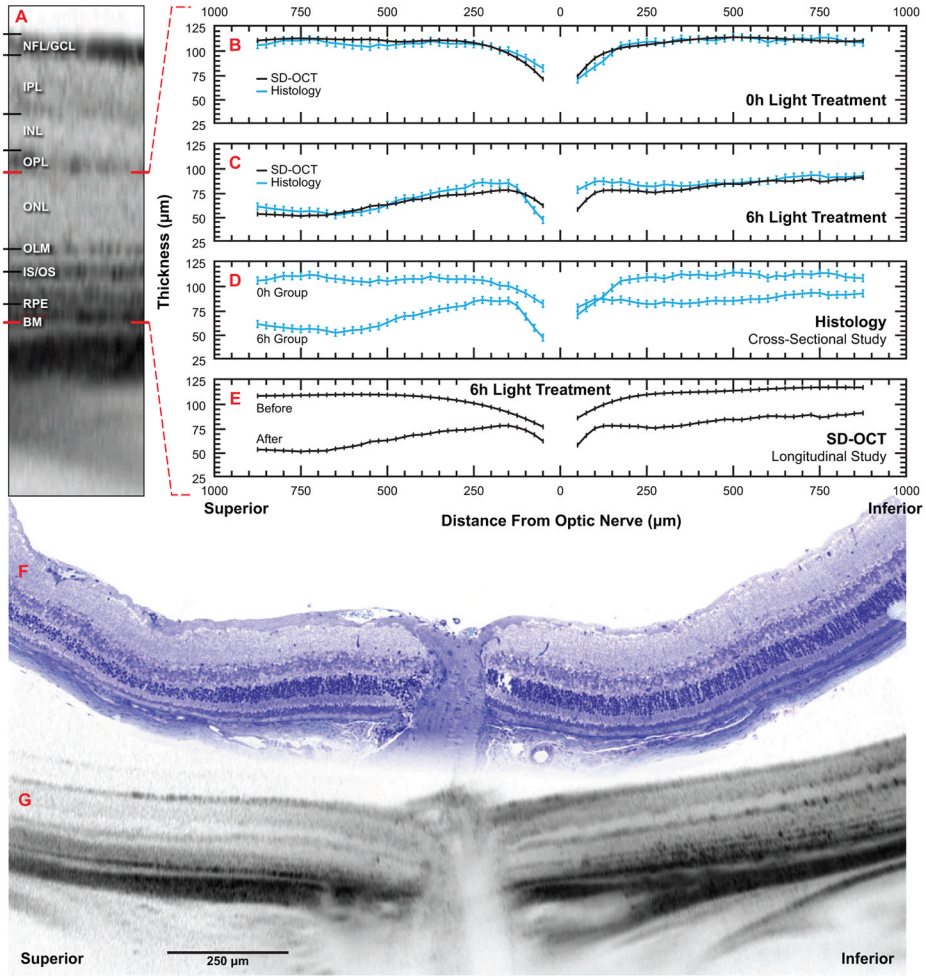

Figure 1.

SD-OCT measurements from mouse retinas emulate histomorphometric data from the same animals. Balb/c mice were initially examined by SD-OCT and their outer retinal thickness determined. Following 10 days recovery from 6 hours bright-light treatment, outer retinal thickness was determined from follow-up SD-OCT examinations and from histologic sections of the same retinas. Another set of mice given 0 hours bright-light treatment were similarly examined. **A**) Tomographic image of a Balb/c mouse retina highlighting morphological retinal layers discernible by SD-OCT. *NFL/GCL*, nerve fiber layer/ganglion cell layer; *IPL*, inner plexiform layer; *INL*, inner nuclear layer; *OPL*, outer plexiform layer; *ONL*, outer nuclear layer; layers are delimited by lines immediately above and below each respective label. *OLM*, outer limiting membrane; *IS/OS*, photoreceptor inner segment / outer segment junction; *RPE*, retinal pigment epithelium; *BM*, Bruch's membrane; features are denoted by the line immediately left of the respective label. Red lines delimit outer retinal layer, as measured in this study, from the base of the photoreceptors to Bruch's membrane. **B**-**E**) Scatter plots of outer retinal thickness along the vertical meridian through the optic nerve; red dashed lines refer back to outer retinal layer as described in **A**; black lines represent mean thickness determined by SD-OCT, blue lines represent mean thickness determined by histology, vertical bars represent ± sem. **B**) SD-OCT and histological comparison of mouse outer retinal thickness following 10 days recovery from 0 hours bright-light treatment. Notice the high degree of overlap between SD-OCT and histological values. **C**) SD-OCT and histological comparison of mouse outer retinal thickness following

10 days recovery from 6 hours bright-light treatment. SD-OCT and histologic values overlap considerably at distances greater than 250 μm beyond the optic nerve. **D**) Conventional cross-section approach to comparing treatments (0 and 6 hours bright-light) by histology. Following 6 hours bright-light treatment, superior and inferior hemispheres exhibit decreases in outer retinal thickness (superior having the greatest loss). Treatments are indistinguishable near the optic nerve in the inferior hemisphere. **E**) Longitudinal approach to the same comparison as in **D**. Rather than comparing treatments groups as in **D**, initial and follow-up exams of the same retinas were used to determine treatment effect on outer retinal thickness within the same animal. Here, the treatment effect is clearly distinguishable at all locations. **F, G**) Representative composite images from the same mouse retina from 6-hour bright-light treatment group illustrating region of analysis in **B-E**. Scale bar and hemisphere annotations apply to both **F** and **G. F**) Tile mosaic of a sequence of high-resolution microscope images of toluidene blue-stained, 1 um-thick plastic section. **G**) Montage of three SD-OCT scans.

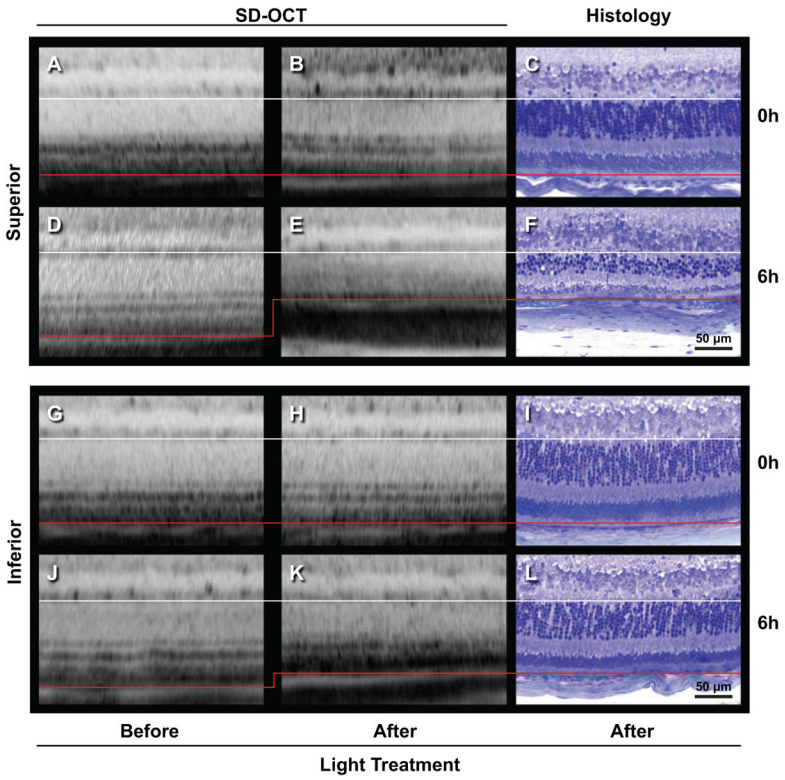

Figure 2.

Representative images demonstrate that SD-OCT emulates histomorphometry. Balb/c mice were examined initially by SD-OCT and their outer retinal thickness was determined. Following 10 days recovery from 6 hours bright-light treatment, outer retinal thickness was determined from follow-up SD-OCT examinations and from histologic sections of the same retinas. Another set of mice given 0 hours bright-light treatment were similarly examined. Lines delimit outer retinal layer, as measured in this study, from the base of the photoreceptors (white line) to Bruch's membrane (red line). Since SD-OCT software algorithms present the retina as straight objects and histological sections have a curved surface, lines were matched at the left of each image. All images display retina approximately 500 μm from the optic nerve. **A-F**) Superior hemisphere. **G-L**) Inferior hemisphere. **A-C, G-I**) Same retina from a 0 hour bright-light treated mouse. **D-F, J-L**) Same retina from a 6-hour bright-light treated mouse. **A, D, G, J**) Initial SD-OCT scans. **B, E, H, K**) Follow-up SD-OCT scans after treatment. **C, F, I, L**) Histologic sections acquired after follow-up SD-OCT scan. Notice shift in red line as outer retinal thickness decreases under 6-hour bright-light treatment (**D** to **E**, **J** to **K**).

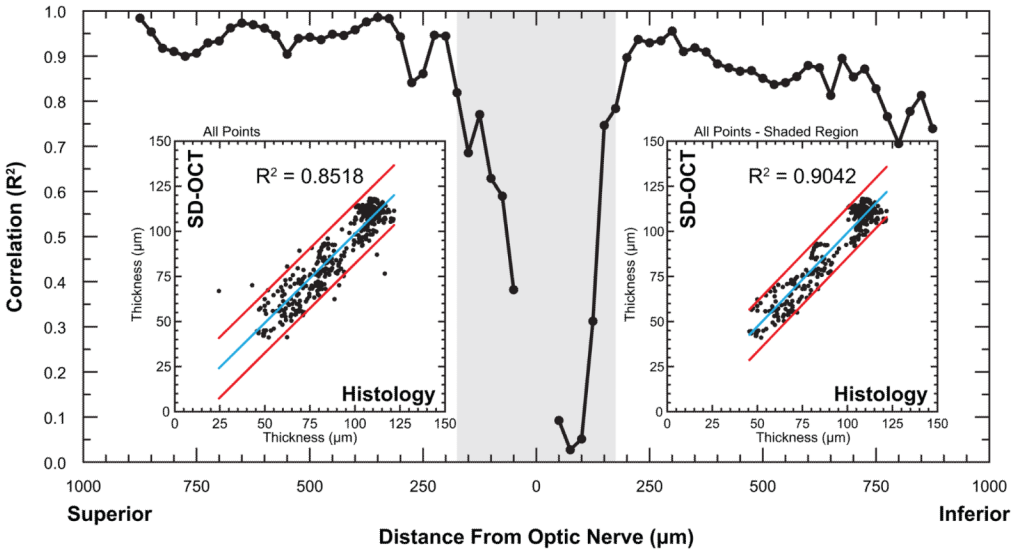

Figure 3.

Outer retinal thickness values determined by SD-OCT correlate with histomorphometric measurements from the same retina. Thickness was measured at 20 µm intervals along the vertical meridian through the optic nerve in histologic sections and across the full length of SD-OCT scans (~950 µm). Measurements were interpolated at 25 µm intervals then compared by simple linear regression as a function of distance from the optic nerve. Shaded region indicates the area of low correlation near the optic nerve. **Insets:** Regression plots of outer retinal thickness determined by SD-OCT and histology; regression line (blue line); 95% confidence limits (red lines). **Left inset:** All data points show an overall correlation of $R^2 = 0.8518$; **Right inset:** Exclusion of data points adjacent to optic nerve (shaded region) reveals that overall correlation increases to $R^2 = 0.9042$.